Phosphorylation of the N-terminus of Syntaxin-16 controls interaction with mVps45 and GLUT4 trafficking in adipocytes

Shaun K Bremner [Corresp., 1] , **Rebecca Berends** [2] , **Alexandra Kaupisch** [2] , **Jennifer Roccisana** [2] , **Calum Sutherland** [3] , **Nia J Bryant** [4] , **Gwyn W Gould** [5]

[1] University of Strathclyde, Glasgow, United Kingdom

[2] Institute of Molecular, Cell and Systems Biology, University of Glasgow, Glasgow, United Kingdom

[3] Department of Cellular Medicine, University of Dundee, Dundee, United Kingdom

[4] Department of Biology, University of York, York, United Kingdom

[5] SIPBS, University of Strathclyde, Glasgow, United Kingdom

Corresponding Author: Shaun K Bremner
Email address: shaun.bremner@strath.ac.uk

The ability of insulin to stimulate glucose transport in muscle and fat cells is mediated by the regulated delivery of intracellular vesicles containing glucose transporter-4 (GLUT4) to the plasma membrane, a process known to be defective in disease such as Type 2 diabetes. In the absence of insulin, GLUT4 is sequestered in tubules and vesicles within the cytosol, collectively known as the GLUT4 storage compartment. A subset of these vesicles, known as the 'insulin responsive vesicles are selectively delivered to the cell surface in response to insulin. We have previously identified Syntaxin16 (Sx16) and its cognate Sec1/Munc18 protein family member mVps45 as key regulatory proteins involved in the delivery of GLUT4 into insulin responsive vesicles. Here we show that mutation of a key residue within the Sx16 N-terminus involved in mVps45 binding, and the mutation of the Sx16 binding site in mVps45 both perturb GLUT4 sorting, consistent with an important role of the interaction of these two proteins in GLUT4 trafficking. We identify Threonine-7 (T7) as a site of phosphorylation of Sx16 *in vitro*. Mutation of T7 to D impairs Sx16 binding to mVps45 *in vitro* and overexpression of T7D significantly impaired insulin-stimulated glucose transport in adipocytes. We show that both AMP-activated protein kinase (AMPK) and its relative SIK2 phosphorylate this site. Our data suggest that Sx16 T7 is a potentially important regulatory site for GLUT4 trafficking in adipocytes.

Phosphorylation of the N-terminus of Syntaxin-16 controls interaction with mVps45 and GLUT4 trafficking in adipocytes.

Shaun K. Bremner[1,*], Rebecca Berends[2], Alexandra Kaupisch[2], Jennifer Roccisana[2], Calum Sutherland[3], Nia J. Bryant[4] and Gwyn W. Gould[1].

[1]Strathclyde Institute of Pharmacy and Biomedical Sciences, University of Strathclyde, Glasgow G4 0RE. United Kingdom.

[2]Institute of Molecular Cell and Systems Biology, CMVLS, University of Glasgow, Glasgow G12 8QQ. United Kingdom.

[3]Cellular Medicine, University of Dundee, Dundee DD1 9SY. United Kingdom.

[4]Department of Biology, University of York, Heslington, York YO10 5DD. United Kingdom.

*Correspondence to: Shaun Bremner. Strathclyde Institute of Pharmacy and Biomedical Sciences, University of Strathclyde, Glasgow G4 0RE. United Kingdom.
shaun.bremner@strath.ac.uk

Abstract

The ability of insulin to stimulate glucose transport in muscle and fat cells is mediated by the regulated delivery of intracellular vesicles containing glucose transporter-4 (GLUT4) to the plasma membrane, a process known to be defective in disease such as Type 2 diabetes. In the absence of insulin, GLUT4 is sequestered in tubules and vesicles within the cytosol, collectively known as the GLUT4 storage compartment. A subset of these vesicles, known as the 'insulin responsive vesicles are selectively delivered to the cell surface in response to insulin. We have previously identified Syntaxin16 (Sx16) and its cognate Sec1/Munc18 protein family member mVps45 as key regulatory proteins involved in the delivery of GLUT4 into insulin responsive vesicles. Here we show that mutation of a key residue within the Sx16 N-terminus involved in mVps45 binding, and the mutation of the Sx16 binding site in mVps45 both perturb GLUT4 sorting, consistent with an important role of the interaction of these two proteins in GLUT4 trafficking. We identify Threonine-7 (T7) as a site of phosphorylation of Sx16 *in vitro*. Mutation of T7 to D impairs Sx16 binding to mVps45 *in vitro* and overexpression of T7D significantly impaired insulin-stimulated glucose transport in adipocytes. We show that both AMP-activated protein kinase (AMPK) and its relative SIK2 phosphorylate this site. Our data

36 suggest that Sx16 T7 is a potentially important regulatory site for GLUT4 trafficking in
37 adipocytes.

Introduction

39 The regulation of glucose transport is a central facet of insulin action (Saltiel 2021;
40 Santoro et al. 2021). Upon insulin binding its receptor, intracellular GLUT4-containing
41 vesicles are rapidly mobilised to the cell surface where they dock and fuse, resulting in
42 increased levels of GLUT4 in the plasma membrane and a consequent increase in
43 glucose transport (Gould et al. 2020; Klip et al. 2019; Santoro et al. 2021).

44 Key to this effect of insulin is the ability of fat and muscle to sequester GLUT4 in tubules
45 and vesicles throughout the cytoplasm which are collectively referred to as the GLUT4
46 storage compartment (GSC) (Bogan & Kandror 2010; Gould et al. 2020). A subfraction
47 of the GSC, generally referred to as insulin-sensitive intracellular vesicles (IRVs), is
48 selectively mobilized by insulin to the plasma membrane (Bogan & Kandror 2010; Klip
49 et al. 2019). The trafficking itinerary of GLUT4 in insulin-sensitive cells has been the
50 subject of significant research. In the absence of insulin GLUT4 is sequestered
51 intracellularly by the coordinated action of two intracellular trafficking pathways (Bryant
52 et al. 2002; Klip et al. 2019). The first operates between the plasma membrane and
53 recycling endosomes and serves to efficiently internalize GLUT4. GLUT4 is then sorted
54 from this pathway into a second cycle that operates between recycling endosomes, the
55 *trans* Golgi network (TGN) and IRVs. Many of the molecules involved in these sorting
56 pathways have been defined, but their regulation is less well understood (Gould et al.
57 2020; Klip et al. 2019).

58 Patients with T2DM exhibit impaired insulin-stimulated glucose transport in muscle and
59 fat; many studies have supported the hypothesis that GLUT4 sorting and/or trafficking
60 are impaired in these patients (Bogan & Kandror 2010; Garvey & Birnbaum 1993;
61 Garvey et al. 1998; Garvey et al. 1993; Hunter & Garvey 1998; Livingstone et al. 2022).
62 For example, GLUT4 is mis-sorted into a denser membrane fraction in muscles from
63 patients with T2DM compared to controls, and insulin does not promote mobilization of
64 GLUT4 from this fraction to the PM (Garvey et al. 1998). Consistent with this, recent
65 work has revealed reduced expression of key proteins involved in GLUT4 sorting in
66 muscle of obese diabetic patients compared to weight-matched controls (Livingstone et
67 al. 2022). Similarly, defective GLUT4 sorting in adipocytes isolated from patients with
68 T2DM (Garvey & Birnbaum 1993) and with gestational diabetes (Garvey et al. 1993)
69 has been described. Consequently, there is an imperative to understand how the
70 trafficking of GLUT4 into IRVs is regulated.

71 Communication between intracellular membrane compartments by vesicle trafficking
72 uses components of the SNARE machinery (Sudhof & Rothman 2009). Studies from
73 several groups, including our own, have identified Syntaxin 16 (Sx16) as a key Q_a-

74 SNARE involved in GLUT4 trafficking towards IRVs (Bremner et al. 2022; Perera et al.
75 2003; Proctor et al. 2006; Shewan et al. 2003). Knockdown or knock-out of Sx16
76 impairs insulin-stimulated glucose transport and results in a reduction in GLUT4 levels
77 (Bremner et al. 2022; Proctor et al. 2006). Q_a-SNAREs are regulated by interaction with
78 members of the Sec1/Munc18 (SM) family (Sudhof & Rothman 2009); Sx16 binds the
79 SM protein mVps45 (Tellam et al. 1997), a protein also required for sorting of GLUT4
80 into IRVs (Roccisana et al. 2013). This interaction is complex however, and likely
81 involves multiple 'modes' of interaction between the Q_a SNARE and the SM protein
82 (Munson & Bryant 2009). In the case of the yeast homologues of Sx16 and mVps45
83 (Tlp2p and Vps45p, respectively) the interaction of Tlg2p with Vps45 involves a high
84 affinity interaction between the N-terminus of the Q_a SNARE with a hydrophobic 'pocket'
85 on the surface of Vps45 which is essential for the formation of productive SNARE
86 complexes (Carpp et al. 2006; Furgason et al. 2009; Struthers et al. 2009).

87 Previously published data suggested that Sx16 and mVps45 act together in GLUT4
88 sorting (Bremner et al. 2022; Proctor et al. 2006; Roccisana et al. 2013). How the
89 interaction between these proteins is regulated, and contributes to their function,
90 remains to be determined, but it is of note that we have previously shown that Sx16 is a
91 phosphoprotein (Perera et al. 2003), and that levels of Sx16 are significantly reduced in
92 obese patients with Type-2 diabetes compared to obese, non-diabetic individuals
93 (Livingstone et al. 2022).

94 Here we show that interaction between Sx16 and mVps45 is required for the effective
95 sorting of GLUT4 in adipocytes and that this interaction may be regulated by
96 phosphorylation of Sx16 in the N-terminal regulatory domain. We identify Threonine-7
97 (T7) as a site of phosphorylation of Sx16 *in vitro* and show over-expression of Sx16
98 containing the phosphomimetic T7D mutation in 3T3-L1 adipocytes significantly
99 impaired insulin-stimulated glucose transport. These and other data argue that the N-
100 terminus of Sx16 is a potential regulatory site for the control of GLUT4 sorting in
101 adipocytes. Finally, we show that both AMP-activated protein kinase (AMPK) and its
102 relative SIK2 phosphorylate this site suggesting that T7 is a potentially important
103 regulatory site for GLUT4 trafficking in adipocytes.

104

Materials and Methods.

Cells and antibodies.

107 HEK293T cells (Cat# CRL-3216 RRID:CVCL_0063) and 3T3-L1 fibroblasts (Cat# CCL-
108 92.1, RRID:CVCL_0123) were obtained from the American Tissue Culture Collection
109 and grown and differentiated into adipocytes as outlined in (Sadler et al. 2019). HeLa
110 cells expressing HA-GLUT4-GFP were as described previously (Morris et al. 2020).
111 AMPK α1/α2 knockout mouse embryonic fibroblasts (MEFs) and control MEFs were

112 cultured as described previously (Laderoute et al. 2006). Antibodies used: anti-GLUT4
113 (Thermo Fisher Scientific Cat# PA1-1065, RRID:AB_2191454), anti-Sx16 (Synaptic
114 Systems Cat# 110 162, RRID:AB_887799), anti-mVps45 (Novus Cat# NB100-2431,
115 RRID:AB_2272935), anti-VAMP4 (Synaptic Systems Cat# 136 002, RRID:AB_887816),
116 anti-SNAP23 (Synaptic Systems Cat# 111 202, RRID:AB_887788) and anti-Syntaxin 4
117 (Synaptic Systems Cat# 110 042, RRID:AB_887853). A phospho-specific antibody
118 raised in rabbits against the N-terminal 16 amino acids of murine Sx16 with Thr-7
119 chemically phosphorylated and recognizing Thr-7 in the Sx16 N-terminus only when
120 phosphorylated, was generated by Antagene Inc (Mountain View, Ca) and purified using
121 affinity chromatography. Anti-AKT (pan) (Cell Signaling Technology Cat# 2920,
122 RRID:AB_1147620) and anti-AKT Phospho-S473 (Cell Signaling Technology
123 Cat#4058), RRID:AB_331168) were used as outlined (Bremner et al. 2022).

124 ***Plasmids and viruses.***

125 HA-GLUT4-GFP in the pRRL-PGK plasmid was from Cynthia Mastick (Brewer et al.
126 2011; Muretta & Mastick 2009) and pCOG70, driving the over-expression of Vps45p
127 harboring an HA tag at its carboxy terminus was a generous gift of Dr. Lindsay Carpp
128 (Carpp et al. 2006; Carpp et al. 2007). The V107R (Sx16 binding deficient) mutant of
129 mVps45 (corresponding to V107R) was generated using a QuickChange kit
130 (ThermoFisher UK) and fully sequenced on both strands prior to expression in yeast.
131 T7A and T7D mutants in a truncated Sx16 lacking the transmembrane domain were
132 generated by PCR and fully sequenced. Constructs comprising the first 33 residues of
133 Sx16 (either wild-type or containing the F10A mutation previously shown to disrupt
134 binding to mVps45) fused to Protein-A were generated by PCR and fully sequenced on
135 both strands and sub-cloned into pcDNA3.1 for expression in mammalian cells. All other
136 cDNAs were as previously outlined (Morris et al. 2020; Proctor et al. 2006; Sadler et al.
137 2019) . Full length Sx16 containing the T7A to T7D mutations were synthesised by
138 GenScript (Piscataway, NJ) and sub-cloned into pCDH vectors for lentivirus production
139 using the ViraPower™ Lentiviral system (Invitrogen) following manufacturer's
140 instructions. The sequence used corresponds to Q8BVI5 in UniProt and is the largest of
141 the proposed splice variants of Sx16 in mouse tissues, and is the only version thought
142 to contain a transmembrane domain. 3T3-L1 adipocytes were incubated with lentivirus
143 for 12h on day 5 or 6 post-differentiation. The media was changed, and the cells were
144 assayed between day 7 and 9 after differentiation (48-72h post infection).

145 ***Recombinant protein production.***

146 Sx16 lacking its transmembrane domain, or the T7A or T7D mutants, were sub-cloned
147 in-frame with dual protein-A tags, expressed in *E. coli* and purified on IgG-Sepharose
148 (GE Healthcare). Protein levels were determined using Micro-BCA kits (Pierce, UK).

149 ***2-deoxyglucose transport, adipocyte fractionation, immunofluorescence, and***
150 ***immunoblotting.***

151 2-Deoxy-D-glucose transport was assayed in cells exactly as outlined (Bremner et al.
152 2022; Roccisana et al. 2013) in except 96-well plates were employed to minimise virus
153 requirements. To determine the levels of GLUT4, adipocyte lysates were generated as
154 outlined (Roccisana et al. 2013; Sadler et al. 2019). SDS-PAGE and immunoblotting
155 were performed as described (Sadler et al. 2019). Immunoblot signals were quantified
156 using LICOR software (Bremner et al. 2022). Immunofluorescence to quantify cell
157 surface GLUT4 staining in HeLa cells was performed exactly as outlined in (Morris et al.
158 2020). Confocal microscopy of HA-GLUT4-GFP-expressing cells was performed on a
159 Zeiss Exciter equipped with a 63x lens (Morris et al. 2020). Images were captured and
160 processed using Zeiss software.

161 ***Phosphorylation and analysis***

162 Adipocyte cytosol was prepared from day-10 adipocytes. Cell plates were washed three
163 times in ice-cold buffer with protease inhibitors (50 mM Hepes pH 7.4; 5 mM EDTA, 10
164 mM sodium pyrophosphate, 10 mM NaF, 150 mM NaCl, 2 mM sodium orthovanadate,
165 50 mM beta-glycerophosphate and 1 mM DTT) and homogenised by passing through a
166 needle twenty times. The homogenate was centrifuged at 12,000 g for ten minutes and
167 the fat cake carefully aspirated. The supernatant was used in a series of *in vitro* kinase
168 assays; supernatant was stored at -80°C prior to use. In brief, ~30 µg of cytosol extract
169 was incubated in 50mM HEPES pH 7.5, 10 mM $MgCl_2$, 2 mM $MnCl_2$, 0.2 mM DTT,
170 50µM ATP.Mg^{2+} ($\pm$ [γ-^{32}P]-ATP) in the presence of 5 µg of recombinant Protein A-
171 tagged Sx16 (residues 1-279 of Sx16, fused to two copies of Protein-A via a thrombin
172 cleavage site), protein A alone or myelin basic protein at 30°C for 2h. Samples were
173 analysed by autoradiography.

174 Analysis of the phosphorylation sites was performed at the FingerPrints facility,
175 University of Dundee. Phosphorylation reactions were carried out exactly as outlined
176 above but using non-radioactive ATP; control reactions lacking cytosol and/or ATP were
177 performed. Bands corresponding to Sx16-PrA were excised and trypsinised, followed by
178 liquid chromatography-electrospray ionisation mass spectrometry on an ABI QTrap
179 4000 instrument. Potential phospho-peptide ions present in samples but absent from
180 controls were submitted to ESI-MS/MS to determine their amino acid sequence and
181 locate the phosphorylated residue.

182 2 µg of purified ProteinA-Sx16 or Protein A-Sx16-T7A was incubated with the indicated
183 purified recombinant protein kinases (5 mU; see figure legends for details) in the
184 presence of 10 mM $MgCl_2$, 0.1 mM [γ-^{32}P]-ATP (approx. 0.5×10^6 cpm/nmol) and kinase
185 buffer (50 mM Tris-Cl, 0.03% (v/v) Brij-35, 0.1% (v/v) β-mercaptoethanol) at 30°C in a
186 total volume of 50 µl. A 20 µl aliquot of reaction mix was taken at the times indicated on

187   the figure legends and the reactions terminated by addition of 4xNovex SDS PAGE
188   loading buffer and heating at 70°C for 15 mins. The Sx16 was separated from [γ-^{32}P]-
189   ATP by SDS-PAGE on Novex 4-12% gradient gels using a MOPS buffer. After staining
190   with Coomassie Brilliant Blue to visualise the protein bands, the gels were dried and
191   subjected to autoradiography. Finally, the Sx16 bands were excised, and the
192   incorporated radioactivity was determined by scintillation counting.

193   In experiments using anti-phospho-T7 for detection, *in vitro* kinases assays typically
194   contained 0.5 mg of bacterially expressed Sx16 incubated with 30 mg of cytosol in the
195   presence or absence of 25 mM ATP for 60 minutes at 30°C as indicated. Samples were
196   then immunoblotted with anti-Sx16 antibodies or anti-phospho-T7 antibodies as
197   described in the figure legends.

198   ***Statistical Analysis***

199   Result are expressed as ± SD with the N-number indicated. Significant differences were
200   determined using either t-test or ANOVA as indicated in the figure legends, with p <
201   0.05 being deemed as significant. Statistical analysis was carried out using GraphPad
202   Prism software.

203

204   **Results.**

205   ***Interaction of mVps45 and Sx16 is functionally important for GLUT4 sorting.***

206   Syntaxin proteins are subject to regulation by cognate SM proteins through multiple
207   distinct but evolutionarily conserved binding mechanisms (Morey et al. 2017; Munson &
208   Bryant 2009; Sudhof & Rothman 2009; Yu et al. 2013). One of the best characterized
209   examples of this is binding of yeast Vps45p by the Syntaxin Tlg2p via its N-terminal
210   peptide which is necessary for productive SNARE complex formation (Carpp et al.
211   2006; Carpp et al. 2007; Furgason et al. 2009; Struthers et al. 2009). This binding
212   mechanism is conserved for mammalian Sx16 which binds mVps45 in an analogous
213   manner (Struthers et al. 2009) and involves the insertion of the Sx16 N-terminus into a
214   hydrophobic pocket located on the surface or mVps45 (Carpp et al. 2006; Dulubova et
215   al. 2002; Munson & Bryant 2009). This interaction is known to mask a lower affinity but
216   functionally important interaction which does not involve the Sx16 N-terminus and
217   involves Sx16 binding to mVps45 in a conformation incompatible with productive
218   SNARE complex formation (Furgason et al. 2009; Munson & Bryant 2009; Struthers et
219   al. 2009).

220   Given the previously demonstrated a role for both Sx16 and mVps45 in GLUT4 traffic
221   (Bremner et al. 2022; Proctor et al. 2006; Roccisana et al. 2013; Shewan et al. 2003),
222   here we asked whether the interaction between these two proteins is required for their
223   function(s) in this process. To this end, we undertook two different approaches to
224   disrupt this interaction. We produced a protein fusion between the N-terminal 33

225 residues of Sx16 and Protein-A and expressed this in HeLa cells expressing HA-
226 GLUT4-GFP. We reasoned that introduction of this N-terminal peptide into cells would
227 inhibit the interaction between Sx16 and mVps45, prevent functional SNARE complex
228 formation and perturb GLUT4 trafficking to the IRVs (Munson & Bryant 2009) and
229 elected to study this initially using the readily tractable HeLa cell system which we and
230 others have shown behaves similarly to adipocytes and muscle (Bryant & Gould 2020;
231 Morris et al. 2020). Consistent with this, we observed significantly reduced insulin-
232 stimulated translocation of HA-GLUT4-GFP to the plasma membrane in cells staining
233 positive for the Protein-A fusion. By contrast, a mutation in this peptide (F10A),
234 previously shown to reduce binding of Sx16/Tlg2p to mVps45/Vps45p (Dulubova et al.
235 2002; Struthers et al. 2009), was without effect (Figure 1A,B).

236 Studies in yeast have shown that mutation of a conserved hydrophobic residue
237 predicted to be on the outer surface of Vps45 is required for interaction with the N-
238 peptide of Tlg2 and Sx16, with its mutation abrogating interaction (Carpp et al. 2006;
239 Dulubova et al. 2002; Struthers et al. 2009). We therefore created this mutation in
240 mVps45 and determined its effect on GLUT4 distribution. The rationale for this
241 approach being that if cycles of association/dissociation of mVps45/Sx16 are needed for
242 effective GLUT4 sorting, the over-expression of a mutant defective in this interaction
243 should manifest itself by impairment of GLUT4 sorting. Transient over-expression of
244 (V107R)-mVps45 in HeLa cells increased cell surface GLUT4 levels measured in the
245 absence of insulin, detected using anti-HA antibodies in non-permeabilised cells,
246 consistent with disruption of the Sx16/mVps45 interaction perturbing trafficking of
247 GLUT4. Over-expression of wild type mVps45 was without effect. This data is shown in
248 Figure 2 in which cells over-expressing wild-type HA-mVps45 or (V107R)-mVps45 were
249 identified by immunostaining with anti mVps45 (we are unable to use anti-HA to quantify
250 mVps45 expression because of the presence of HA-tagged GLUT4 in these cells). This
251 approach stains both endogenous and over-expressed proteins, hence in the visual
252 analysis shown, cells expressing higher than average mVps45 staining were assigned
253 to be positive for the transfected DNA (Figure 2A); similar levels of the mVps45 species
254 were expressed as judged by immunoblot analysis (Figure 2B). To mitigate against bias
255 in this subjective analysis, we also measured the cell surface GLUT [HA staining in non-
256 permeabilised cells]/GFP ratio for entire populations of transfected cells (i.e., containing
257 both non-transfected and transfected cells) and found that over-expression of wild-type
258 HA-mVps45 did not change the cell surface GLUT[HA staining in non-permeabilised
259 cells]/GFP ratio compared to non-transfected cells, but over-expression of (V107R)-
260 mVps45 consistently increased this ratio by 20% (Figure 2C). Collectively, these data,
261 together with our previous observations of depletion of either protein separately
262 (Bremner et al. 2022; Proctor et al. 2006; Shewan et al. 2003), supports the hypothesis
263 that an interaction between the N-terminus of Sx16 and mVps45 is required for the
264 correct trafficking of GLUT4.

Sx16 is phosphorylated on T7

Previous work from this lab has shown that Sx16 is a phosphoprotein (Perera et al. 2003). We therefore sought to identify potential sites of phosphorylation of this key SNARE. Attempts to identify phosphosites using combinations of co-IP or purification from adipocytes proved unsuccessful. However, we consistently observed phosphorylation of recombinant Sx16 *in vitro* using an adipocyte cytosolic extract (Figure 3A). Therefore, this phosphorylated recombinant Sx16 was subjected to phospho-site mapping. Phospho-mapping hits (FingerPrints ProteomicsFacility, University of Dundee) were assigned a score based upon probabilities that the fragment detected was a true phospho-peptide (Table 1; Supplemental Figure 1). The highest score, and the only hit, was assigned to fragments containing Threonine-7 (hereafter T7) suggesting that under these conditions, T7 is a major phospho-acceptor site. We therefore generated a phospho-selective antibody against the N-terminal 16 amino acids of murine Sx16. This antibody recognized a band of the expected molecular weight in *in vitro* phosphorylation reactions, the intensity of which increased significantly when ATP was included in the reactions (Figure 3B). Consistent with this antibody recognising the phosphorylated forms of Sx16, we showed that the antibody cross-reacted strongly with recombinant Sx16-T7D but significantly less so with Sx16-T7A or Sx16 purified from bacteria (Figure 3C).

Phospho-mimetic mutation of T7 perturbs binding to mVps45.

Interaction of Sx16 with mVps45 involves the extreme N-terminus of Sx16 (Carpp et al. 2006; Dulubova et al. 2002; Furgason et al. 2009; Munson & Bryant 2009), hence the identification of a potential phospho-acceptor site in this region could suggest a potential regulatory mechanism to control Sx16/mVps45 interaction and function. To test this, we employed recombinant Sx16-PrA to pull-down HA-tagged human mVps45 expressed in yeast and compared wildtype Sx16 (which is not phosphorylated when expressed in bacteria) with Sx16-PrA containing the phospho-mimetic T7D mutation (Figure 4). As shown wild-type Sx16 effectively pulled-down HA-tagged mVps45 from yeast lysate. Although Sx16-T7D was still able to bind HA-mVps45, this was reduced in both magnitude and affinity (Figure 4). This data strongly suggests that phosphorylation of T7 could significantly impact Sx16 function by preventing or reducing the affinity of its interaction with mVps45.

Sx16-T7D perturbs insulin-stimulated glucose transport

Previously, we have shown that perturbation of either Sx16 or mVps45 function modulated GLUT4 sorting in adipocytes. Hence, if the interaction between Sx16 and mVps45 is regulated by phosphorylation at T7, as suggested by the data in Figures 3 and 4, we would predict that phosphorylation of this site would be expected to modulate GLUT4 trafficking *in vivo*.

303 To test this hypothesis, full length Sx16 wild-type, or T7A and T7D mutants were over-
304 expressed in 3T3-L1 adipocytes, a well-used model of insulin-stimulated GLUT4
305 translocation and glucose transport. We consistently observed reduced insulin-
306 stimulated 2-deoxyglucose uptake in cells over-expressing Sx16-T7D compared to
307 either wild-type or Sx16-T7A (Figure 5A). To facilitate comparison of datasets from
308 biological replicates in which levels of over-expression of Sx16 varied and the
309 magnitude of the insulin response varied, the data from multiple experiments expressed
310 as a % of the maximal insulin response is shown in Figure 5A. A representative
311 immunoblot of lysates from a typical experiment is shown in Figure 5B; for reasons that
312 we have been unable to identify, the overexpressed proteins migrate faster than
313 endogenous Sx16. The apparent reduction in total GLUT4 levels in T7D-expressing
314 cells in this dataset was not recapitulated consistently in all experiments. Importantly,
315 insulin-stimulated activation of Akt was not modulated by expression of the different
316 Sx16 mutants, indicating that a deficit in insulin-signalling is unlikely to be the
317 mechanism responsible for reduced insulin-simulated glucose transport (Figure 5C).

318 ***Sx16 is a substrate for AMP-dependent protein kinase.***

319 The observation that Sx16-T7 is a potential regulatory site for the control of GLUT4
320 trafficking prompted an investigation of the kinase(s) that might phosphorylate this site.
321 The peptide sequence around T7 resembles the proposed consensus sequence for the
322 AMP activated protein kinase (AMPK) and several of its related kinases (Bright et al.
323 2009). AMPK activation enhances insulin-stimulated glucose transport in skeletal
324 muscle (Kleinert et al. 2017). However, it should be noted that in 3T3-L1 adipocytes, the
325 converse is true: activation of AMPK inhibits insulin-stimulated glucose transport and
326 GLUT4 translocation to the plasma membrane (Salt et al. 2000). Using recombinant
327 Sx16 as a substrate for *in vitro* phosphorylation reactions revealed that AMPK
328 phosphorylated Sx16 *in vitro*, and that the extent of this phosphorylation was
329 comparatively reduced in Sx16-T7A under identical initial rate phosphorylation
330 conditions. Importantly phosphorylation was enhanced by inclusion of AMP in the
331 kinase assay mix (Figure 6). Sx16 was also phosphorylated by the AMPK-related
332 kinase SIK2 (Bright et al. 2009; Patel et al. 2014) and the extent of this phosphorylation
333 was consistently reduced in the Sx16-T7A mutant (Figure 6); MARK1(Bright et al. 2009)
334 also phosphorylates Sx16 but this was not reduced in Sx16-T7A and hence was not
335 studied further (Supplemental Figure 2). By contrast the AMPK-related kinase BRSK2
336 (Bright et al. 2009) (Supplemental Figure 2) was without effect on Sx16
337 phosphorylation. It should be noted that phosphorylation of Sx16-T7A by AMPK is also
338 observed, indicating that further phospho-acceptor sites are present within this SNARE
339 protein.

340 Our initial report identifying Sx16 as a phosphoprotein indicated that total Sx16
341 phosphorylation levels were slightly reduced in insulin-stimulated 3T3-L1 adipocytes

342 compared to controls (Perera et al. 2003). Hence, we adopted several routes to address
343 this in intact 3T3-L1 adipocytes here focussing on phospho-T7 levels using our
344 phospho-selective antibody. We have been unable to measure any change in phospho-
345 T7 levels in 3T3-L1 adipocytes in response to insulin (Figure 7A) or 5-aminoimidazole-
346 4-carboxamide ribonucleotide (AICAR) a known activator of AMPK, (Figure 7B). One
347 possible explanation for this is provided by the data in Figure 7C in which lysates from
348 Mouse Embryonic Fibroblasts (MEFs) engineered to lack AMPK compared to their
349 wildtype counterparts were used in in vitro phosphorylation reactions with or without the
350 addition of ATP. Lack of AMPK modestly reduced the phosphorylation of Sx16 (Figure
351 7D), but the effect was small, indicating that other, presently unidentified, kinases may
352 regulate this site. This is consistent with the autoradiography in Figure 6 which indicates
353 substantial phosphorylation of Sx16-T7A by AMPK, suggesting that other sites within
354 Sx16 may be important, and with our previous data (Perera et al. 2003). Future work
355 should address whether phosphorylation status of Sx16 is altered in disease or
356 conditions of insulin resistance.

357

358

Discussion.

360 Previous work from our group and others has established a role for Sx16 in the
361 trafficking of GLUT4 (Bremner et al. 2022; Proctor et al. 2006; Shewan et al. 2003).
362 Similarly, we have shown that mVps45, the Sec1/Munc18 protein that is known to bind
363 to Sx16 is also required for this trafficking event (Roccisana et al. 2013). Studies from
364 our group and others has shown that Sx16 binds to mVps45 via the extreme N-terminus
365 of Sx16 inserting into a pocket on the surface of mVps45 (Carpp et al. 2006; Carpp et
366 al. 2007; Munson & Bryant 2009; Struthers et al. 2009). Disruption of either the Sx16 N-
367 terminus or the V107R mVps45 mutant prevents this interaction (Carpp et al. 2006;
368 Dulubova et al. 2002; Shanks et al. 2012; Stepensky et al. 2013). Here we show that
369 perturbation of interaction between these two proteins using a peptide mimetic
370 corresponding to the N-terminal 33 residues of Sx16 reduces insulin-stimulated GLUT4
371 translocation (Figure 1). Further, over-expression of the V107R mutant of mVps45
372 (V107R; Figure 2) also perturbs GLUT4 trafficking in HeLa cells, consistent with an
373 important role for the interaction of these proteins in determining the intracellular fate of
374 GLUT4. It is important to emphasise that these two experiments are distinct:
375 overexpression of the Sx16 N-terminal peptide competes with endogenous Sx16 for
376 binding to mVps45 and thus inhibits *productive* SNARE complex formation (Furgason et
377 al. 2009; Munson & Bryant 2009; Struthers et al. 2009). The mutant form of mVps45-
378 V107R (figure 2) cannot bind the Sx16 N-terminus but can still bind Sx16 in a
379 conformation incompatible with productive SNARE complex formation (Furgason et al.
380 2009; Munson & Bryant 2009; Struthers et al. 2009). As mVps45 cycles on and off

381 membranes and through these different conformational states (Bryant & James 2003),
382 the mechanism underlying the inhibitory effects observed in Figures 1 and 2 is likely
383 distinct. However, these data clearly establish an important role for the interaction of the
384 N-terminus of Sx16 with mVps45 in the sorting of GLUT4 to IRVs.

385 This begs the question of how this interaction might be regulated. Recent work has
386 identified phosphorylation as a potential control mechanism for the function of Q_a-
387 SNARE/Syntaxin family members (Aran et al. 2011; Barak-Broner et al. 2021; Chung et
388 al. 2000; Gurunathan et al. 2002; Liu et al. 2014; Marash & Gerst 2001; Marash & Gerst
389 2003; Tadokoro et al. 2016). Sx3 is constitutively phosphorylated at T14 in mast cells,
390 and this phosphorylation has been shown to regulate the interaction of this Q_a-SNARE
391 with its cognate Sec1/Munc18 protein, Munc18-2 (Tadokoro et al. 2016). Sx1
392 phosphorylation at S14 has also been shown to be a key regulatory event in controlling
393 exocytosis in neuroendocrine cells (Barak-Broner et al. 2021). It is of note that both
394 these proteins are phosphorylated in their N-terminal regulatory domains (MacDonald et
395 al. 2010; Munson & Bryant 2009; Sudhof & Rothman 2009).

396 We (Perera et al. 2003) and others (Fazakerley et al. 2022; Hornbeck et al. 2004)
397 identified Sx16 as a phosphoprotein; using recombinant Sx16 and concentrated
398 adipocyte cytosol, we identified T7 as a potential phospho- acceptor site (Figure 3,
399 Table 1, Supplemental Figure 1). This is intriguing, as this site lies within the domain of
400 Sx16 known to bind mVps45 (Carpp et al. 2006; Dulubova et al. 2002; Furgason et al.
401 2009), and others have suggested that phosphorylation of Sx proteins in this region
402 might modulate SM protein binding (Barak-Broner et al. 2021; Munson & Bryant 2009;
403 Tadokoro et al. 2016). We therefore generated recombinant phospho-mimetic Sx16-
404 T7D and its wild-type counterpart in bacterial and compared their ability to pull-down
405 mammalian mVps45 expressed in yeast. Figure 4 shows that the phospho-mimetic
406 mutant, Sx16-T7D, was significantly impaired in its ability to pull-down mVps45,
407 suggesting that phosphorylation of this site might regulate Sx16/mVps45 interaction and
408 thus impair trafficking events dependent on the productive Sx16/mVs45 interaction.
409 Consistent with this result, studies of the yeast Q_a-SNARE Sso2p have shown that
410 dephosphorylation of this Q_a-SNARE drives the formation of SNARE complex assembly
411 (Gurunathan et al. 2002; Marash & Gerst 2001; Marash & Gerst 2003). This supports
412 our working model in which cycles of phosphorylation/dephosphorylation of Sx16
413 modulate the interaction of Sx16 with mVps45 and thus control trafficking events
414 mediated by these proteins.

415 To further test this hypothesis, we found that over-expression of Sx16-T7D, but not T7A
416 (or wild-type Sx16) impaired insulin stimulated glucose transport in 3T3-L1 adipocytes
417 (Figure 5). Although the magnitude of this inhibition exhibited some variation reflecting
418 different levels of over-expression relative to endogenous Sx16, the T7D mutant
419 consistently impaired insulin-stimulated glucose transport (55 ±16%). This data is

420 consistent with a model in which phosphorylation of the N-terminus of Sx16 prevents
421 the formation of productive SNARE complexes and thus effective sorting of GLUT4 into
422 IRVs. It is important to note that although the affinity of Sx16-T7D for mVps45 is
423 reduced compared to non-phosphorylated Sx16 (Figure 4), the net effect is to reduce
424 the formation of productive SNARE complexes (see discussion above) and thus perturb
425 trafficking of GLUT4 into IRVs (Figure 5). (Bremner et al. 2022; Proctor et al. 2006;
426 Roccisana et al. 2013).

427 This data suggests that phosphorylation of T7 might play a role in the regulation of
428 glucose disposal and thus we sought to identify which kinase(s) may be potential
429 regulators of this site. The peptide sequence around T7 resembles the proposed
430 consensus sequence for the AMP activated protein kinase (AMPK) and several of its
431 related kinases (Bright et al. 2009). Using *in vitro* kinase assays, we show that both
432 AMPK and SIK2 phosphorylate Sx16 *in vitro* (Figure 6); however it is important to note
433 that the data in Figure 6 reveal that Sx16 is probably phosphorylated on multiple sites
434 by AMPK *in vitro*, as Sx16-T7A is phosphorylated by AMPK, albeit to a lesser degree
435 than wildtype Sx16. It should be noted that other AMPK-family members (SIK1, MARK2,
436 NUAK and BRSK2) did not phosphorylate this or indeed other sites in Sx16 (Figure 6).

437 Given the importance of T7 in regulating interaction with mVps45, we used our
438 phospho-specific antibody to ascertain whether there were insulin- or AICAR-driven
439 changes in Sx16 phosphorylation at this site (Figure 7A, B). No significant changes in
440 T7 phosphorylation were observed using cytosol from insulin or AICAR-treated
441 adipocytes. We have previously reported a decrease in Sx16 phosphorylation in
442 response to insulin using immunoprecipitation from adipocytes. It is possible that
443 elements of the regulatory network are not recapitulated using cytosolic extracts of cells,
444 such as those shown in figure 7. It is frustrating that our phospho-specific antibody
445 proved insufficiently discriminatory to study phosphorylation of endogenous Sx16 in
446 whole cell extracts (by way of example, see Figure 7A in lanes lacking recombinant
447 Sx16).Hence it is formally possible that the experimental results reported in Figure 7 do
448 not fully reflect the situation in intact cells. Furthermore, it is possible that the insulin-
449 regulated dephosphorylation of Sx16 observed in Perera et al. is accounted for by
450 changes at sites other than T7.

451 In an effort to ascertain whether AMPK was the predominant kinase for T7, we prepared
452 lysates from MEFs engineered to lack AMPK ('AMPK KO cells') and found that
453 phosphorylation of Sx16 was modestly reduced when using MEFs from AMPK KO cells
454 compared to their wildtype counterparts. While supporting the hypothesis that AMPK
455 phosphorylates Sx16, clearly other potential explanations for this result should be kept
456 in mind, such as inadequate activation of a distinct down-stream AMPK, etc.

457 These caveats notwithstanding, our data raise the interesting possibility that activation
458 of AMPK (a known regulator of glucose transport (Bright et al. 2009; Salt et al. 2000)) or

459   SIK2 could impact GLUT4 sorting by targeting the Sx16/mVps45 interaction. While we
460   did not observe any consistent effect of either insulin or AICAR on Sx16
461   phosphorylation at this site, our data indicates that other, presently unidentified kinases,
462   may target this site and thus further work is required to functionally link phosphorylation
463   of T7 to specific cellular stimuli or diseased states.

464   In sum, our data confirm an important role of Sx16/mVps45 in GLUT4 sorting in
465   adipocytes and reveal that phosphorylation of Sx16 might offer a novel target for
466   therapeutic intervention in Type-2 diabetes.

467

468   ***Acknowledgements.***

469   We thank Drs Douglas Lamont and Kenneth Beattie of the FingerPrints Proteomics
470   Facility, Dundee, for help with the MS analysis and Mike Mao at Antagene for help with
471   the phospho-antibody production. We thank the reviewers of this work for constructive
472   and helpful suggestions.

473

474   **References.**

475   Aran V, Bryant NJ, and Gould GW. 2011. Tyrosine phosphorylation of Munc18c on residue
476   521 abrogates binding to Syntaxin 4. *BMC Biochem* 12:19. 10.1186/1471-2091-12-
477   19
478   Barak-Broner N, Singer-Lahat D, Chikvashvili D, and Lotan I. 2021. CK2 Phosphorylation Is
479   Required for Regulation of Syntaxin 1A Activity in Ca(2+)-Triggered Release in
480   Neuroendocrine Cells. *Int J Mol Sci* 22. 10.3390/ijms222413556
481   Bogan JS, and Kandror KV. 2010. Biogenesis and regulation of insulin-responsive vesicles
482   containing GLUT4. *Curr Opin Cell Biol* 22:506-512. 10.1016/j.ceb.2010.03.012
483   Bremner SK, Al Shammari WS, Milligan RS, Hudson BD, Sutherland C, Bryant NJ, and Gould
484   GW. 2022. Pleiotropic effects of Syntaxin16 identified by gene editing in cultured
485   adipocytes. *Frontiers in Cell and Developmental Biology* 10. ARTN 1033501
486   10.3389/fcell.2022.1033501
487   Brewer PD, Romenskaia I, Kanow MA, and Mastick CC. 2011. Loss of AS160 Akt substrate
488   causes Glut4 protein to accumulate in compartments that are primed for fusion in
489   basal adipocytes. *J Biol Chem* 286:26287-26297. 10.1074/jbc.M111.253880
490   Bright NJ, Thornton C, and Carling D. 2009. The regulation and function of mammalian
491   AMPK-related kinases. *Acta Physiol (Oxf)* 196:15-26. 10.1111/j.1748-
492   1716.2009.01971.x
493   Bryant NJ, and Gould GW. 2020. Insulin stimulated GLUT4 translocation - Size is not
494   everything! *Curr Opin Cell Biol* 65:28-34. 10.1016/j.ceb.2020.02.006
495   Bryant NJ, Govers R, and James DE. 2002. Regulated transport of the glucose transporter
496   GLUT4. *Nat Rev Mol Cell Biol* 3:267-277. 10.1038/nrm782

497   Bryant NJ, and James DE. 2003. The Sec1p/Munc18 (SM) protein, Vps45p, cycles on and off
498   membranes during vesicle transport. *J Cell Biol* 161:691-696.
499   10.1083/jcb.200212078
500   Carpp LN, Ciufo LF, Shanks SG, Boyd A, and Bryant NJ. 2006. The Sec1p/Munc18 protein
501   Vps45p binds its cognate SNARE proteins via two distinct modes. *J Cell Biol*
502   173:927-936. 10.1083/jcb.200512024
503   Carpp LN, Shanks SG, Struthers MS, and Bryant NJ. 2007. Cellular levels of the syntaxin
504   Tlg2p are regulated by a single mode of binding to Vps45p. *Biochem Biophys Res*
505   *Commun* 363:857-860. 10.1016/j.bbrc.2007.09.067
506   Chung SH, Polgar J, and Reed GL. 2000. Protein kinase C phosphorylation of syntaxin 4 in
507   thrombin-activated human platelets. *J Biol Chem* 275:25286-25291.
508   10.1074/jbc.M004204200
509   Dulubova I, Yamaguchi T, Gao Y, Min SW, Huryeva I, Sudhof TC, and Rizo J. 2002. How
510   Tlg2p/syntaxin 16 'snares' Vps45. *EMBO J* 21:3620-3631. 10.1093/emboj/cdf381
511   Fazakerley DJ, van Gerwen J, Cooke KC, Duan X, Needham EJ, Madsen S, Norris DM, Shun-
512   Shion AS, Krycer JR, Burchfield JG, Yang P, Wade MR, Brozinick JT, James DE, and
513   Humphrey SJ. 2022. Phosphoproteomics reveals rewiring of the insulin signaling
514   network and multi-nodal defects in insulin resistance.
515   *bioRxiv*:2022.2005.2026.493198. 10.1101/2022.05.26.493198
516   Furgason ML, MacDonald C, Shanks SG, Ryder SP, Bryant NJ, and Munson M. 2009. The N-
517   terminal peptide of the syntaxin Tlg2p modulates binding of its closed conformation
518   to Vps45p. *Proc Natl Acad Sci U S A* 106:14303-14308. 10.1073/pnas.0902976106
519   Garvey WT, and Birnbaum MJ. 1993. Cellular insulin action and insulin resistance. *Baillieres*
520   *Clin Endocrinol Metab* 7:785-873. 10.1016/s0950-351x(05)80237-x
521   Garvey WT, Maianu L, Zhu JH, Brechtel-Hook G, Wallace P, and Baron AD. 1998. Evidence
522   for defects in the trafficking and translocation of GLUT4 glucose transporters in
523   skeletal muscle as a cause of human insulin resistance. *J Clin Invest* 101:2377-2386.
524   10.1172/JCI1557
525   Garvey WT, Maianu L, Zhu JH, Hancock JA, and Golichowski AM. 1993. Multiple defects in
526   the adipocyte glucose transport system cause cellular insulin resistance in
527   gestational diabetes. Heterogeneity in the number and a novel abnormality in
528   subcellular localization of GLUT4 glucose transporters. *Diabetes* 42:1773-1785.
529   10.2337/diab.42.12.1773
530   Gould GW, Brodsky FM, and Bryant NJ. 2020. Building GLUT4 Vesicles: CHC22 Clathrin's
531   Human Touch. *Trends Cell Biol* 30:705-719. 10.1016/j.tcb.2020.05.007
532   Gurunathan S, Marash M, Weinberger A, and Gerst JE. 2002. t-SNARE phosphorylation
533   regulates endocytosis in yeast. *Mol Biol Cell* 13:1594-1607. 10.1091/mbc.01-11-
534   0541
535   Hornbeck PV, Chabra I, Kornhauser JM, Skrzypek E, and Zhang B. 2004. PhosphoSite: A
536   bioinformatics resource dedicated to physiological protein phosphorylation.
537   *Proteomics* 4:1551-1561. 10.1002/pmic.200300772
538   Hunter SJ, and Garvey WT. 1998. Insulin action and insulin resistance: diseases involving
539   defects in insulin receptors, signal transduction, and the glucose transport effector
540   system. *Am J Med* 105:331-345. 10.1016/s0002-9343(98)00300-3
541   Kleinert M, Parker BL, Fritzen AM, Knudsen JR, Jensen TE, Kjobsted R, Sylow L, Ruegg M,
542   James DE, and Richter EA. 2017. Mammalian target of rapamycin complex 2

543   regulates muscle glucose uptake during exercise in mice. *J Physiol* 595:4845-4855.
544   10.1113/JP274203
545   Klip A, McGraw TE, and James DE. 2019. Thirty sweet years of GLUT4. *J Biol Chem*
546   294:11369-11381. 10.1074/jbc.REV119.008351
547   Laderoute KR, Amin K, Calaoagan JM, Knapp M, Le T, Orduna J, Foretz M, and Viollet B.
548   2006. 5'-AMP-activated protein kinase (AMPK) is induced by low-oxygen and
549   glucose deprivation conditions found in solid-tumor microenvironments. *Mol Cell*
550   *Biol* 26:5336-5347. 10.1128/MCB.00166-06
551   Liu X, Heidelberger R, and Janz R. 2014. Phosphorylation of syntaxin 3B by CaMKII
552   regulates the formation of t-SNARE complexes. *Mol Cell Neurosci* 60:53-62.
553   10.1016/j.mcn.2014.03.002
554   Livingstone R, Bryant NJ, Boyle JG, Petrie JR, and Gould GW. 2022. Diabetes is accompanied
555   by changes in the levels of proteins involved in endosomal GLUT4 trafficking in
556   obese human skeletal muscle. *Endocrinology, Diabetes and Metabolism* in press.
557   MacDonald C, Munson M, and Bryant NJ. 2010. Autoinhibition of SNARE complex assembly
558   by a conformational switch represents a conserved feature of syntaxins. *Biochem*
559   *Soc Trans* 38:209-212. 10.1042/BST0380209
560   Marash M, and Gerst JE. 2001. t-SNARE dephosphorylation promotes SNARE assembly and
561   exocytosis in yeast. *EMBO J* 20:411-421. 10.1093/emboj/20.3.411
562   Marash M, and Gerst JE. 2003. Phosphorylation of the autoinhibitory domain of the Sso t-
563   SNAREs promotes binding of the Vsm1 SNARE regulator in yeast. *Mol Biol Cell*
564   14:3114-3125. 10.1091/mbc.e02-12-0804
565   Morey C, Kienle CN, Klopper TH, Burkhardt P, and Fasshauer D. 2017. Evidence for a
566   conserved inhibitory binding mode between the membrane fusion assembly factors
567   Munc18 and syntaxin in animals. *J Biol Chem* 292:20449-20460.
568   10.1074/jbc.M117.811182
569   Morris S, Geoghegan ND, Sadler JBA, Koester AM, Black HL, Laub M, Miller L, Heffernan L,
570   Simpson JC, Mastick CC, Cooper J, Gadegaard N, Bryant NJ, and Gould GW. 2020.
571   Characterisation of GLUT4 trafficking in HeLa cells: comparable kinetics and
572   orthologous trafficking mechanisms to 3T3-L1 adipocytes. *PeerJ* 8:e8751.
573   10.7717/peerj.8751
574   Munson M, and Bryant NJ. 2009. A role for the syntaxin N-terminus. *Biochem J* 418:e1-3.
575   10.1042/BJ20082389
576   Muretta JM, and Mastick CC. 2009. How insulin regulates glucose transport in adipocytes.
577   *Vitam Horm* 80:245-286. 10.1016/S0083-6729(08)00610-9
578   Patel K, Foretz M, Marion A, Campbell DG, Gourlay R, Boudaba N, Tournier E, Titchenell P,
579   Peggie M, Deak M, Wan M, Kaestner KH, Goransson O, Viollet B, Gray NS, Birnbaum
580   MJ, Sutherland C, and Sakamoto K. 2014. The LKB1-salt-inducible kinase pathway
581   functions as a key gluconeogenic suppressor in the liver. *Nat Commun* 5:4535.
582   10.1038/ncomms5535
583   Perera HK, Clarke M, Morris NJ, Hong W, Chamberlain LH, and Gould GW. 2003. Syntaxin 6
584   regulates Glut4 trafficking in 3T3-L1 adipocytes. *Mol Biol Cell* 14:2946-2958.
585   10.1091/mbc.e02-11-0722
586   Proctor KM, Miller SC, Bryant NJ, and Gould GW. 2006. Syntaxin 16 controls the
587   intracellular sequestration of GLUT4 in 3T3-L1 adipocytes. *Biochem Biophys Res*
588   *Commun* 347:433-438. 10.1016/j.bbrc.2006.06.135

589   Roccisana J, Sadler JB, Bryant NJ, and Gould GW. 2013. Sorting of GLUT4 into its insulin-
590   sensitive store requires the Sec1/Munc18 protein mVps45. *Mol Biol Cell* 24:2389-
591   2397. 10.1091/mbc.E13-01-0011
592   Sadler JBA, Lamb CA, Welburn CR, Adamson IS, Kioumourtzoglou D, Chi NW, Gould GW, and
593   Bryant NJ. 2019. The deubiquitinating enzyme USP25 binds tankyrase and regulates
594   trafficking of the facilitative glucose transporter GLUT4 in adipocytes. *Sci Rep*
595   9:4710. 10.1038/s41598-019-40596-5
596   Salt IP, Connell JM, and Gould GW. 2000. 5-aminoimidazole-4-carboxamide ribonucleoside
597   (AICAR) inhibits insulin-stimulated glucose transport in 3T3-L1 adipocytes.
598   *Diabetes* 49:1649-1656. 10.2337/diabetes.49.10.1649
599   Saltiel AR. 2021. Insulin signaling in health and disease. *J Clin Invest* 131:e142241.
600   10.1172/JCI142241
601   Santoro A, McGraw TE, and Kahn BB. 2021. Insulin action in adipocytes, adipose
602   remodeling, and systemic effects. *Cell Metab* 33:748-757.
603   10.1016/j.cmet.2021.03.019
604   Shanks SG, Carpp LN, Struthers MS, McCann RK, and Bryant NJ. 2012. The Sec1/Munc18
605   protein Vps45 regulates cellular levels of its SNARE binding partners Tlg2 and Snc2
606   in Saccharomyces cerevisiae. *PLoS One* 7:e49628. 10.1371/journal.pone.0049628
607   Shewan AM, van Dam EM, Martin S, Luen TB, Hong W, Bryant NJ, and James DE. 2003.
608   GLUT4 recycles via a trans-Golgi network (TGN) subdomain enriched in Syntaxins 6
609   and 16 but not TGN38: involvement of an acidic targeting motif. *Mol Biol Cell*
610   14:973-986. 10.1091/mbc.e02-06-0315
611   Stepensky P, Saada A, Cowan M, Tabib A, Fischer U, Berkun Y, Saleh H, Simanovsky N,
612   Kogot-Levin A, Weintraub M, Ganaiem H, Shaag A, Zenvirt S, Borkhardt A, Elpeleg O,
613   Bryant NJ, and Mevorach D. 2013. The Thr224Asn mutation in the VPS45 gene is
614   associated with the congenital neutropenia and primary myelofibrosis of infancy.
615   *Blood* 121:5078-5087. 10.1182/blood-2012-12-475566
616   Struthers MS, Shanks SG, MacDonald C, Carpp LN, Drozdowska AM, Kioumourtzoglou D,
617   Furgason ML, Munson M, and Bryant NJ. 2009. Functional homology of mammalian
618   syntaxin 16 and yeast Tlg2p reveals a conserved regulatory mechanism. *J Cell Sci*
619   122:2292-2299. 10.1242/jcs.046441
620   Sudhof TC, and Rothman JE. 2009. Membrane fusion: grappling with SNARE and SM
621   proteins. *Science* 323:474-477. 10.1126/science.1161748
622   Tadokoro S, Shibata T, Inoh Y, Amano T, Nakanishi M, Hirashima N, and Utsunomiya-Tate
623   N. 2016. Phosphorylation of syntaxin-3 at Thr 14 negatively regulates exocytosis in
624   RBL-2H3 mast cells. *Cell Biol Int* 40:589-596. 10.1002/cbin.10600
625   Tellam JT, James DE, Stevens TH, and Piper RC. 1997. Identification of a mammalian Golgi
626   Sec1p-like protein, mVps45. *J Biol Chem* 272:6187-6193. 10.1074/jbc.272.10.6187
627   Yu H, Rathore SS, Lopez JA, Davis EM, James DE, Martin JL, and Shen J. 2013. Comparative
628   studies of Munc18c and Munc18-1 reveal conserved and divergent mechanisms of
629   Sec1/Munc18 proteins. *Proc Natl Acad Sci U S A* 110:E3271-3280.
630   10.1073/pnas.1311232110
631

632   **Supplemental Figure 1.**
633   Original MS spectra of the three species shown in Table 1 are presented.
634
635   **Supplemental Figure 2.**
636   **MARK1 and BRSK2 kinase assays on Sx16.**
637   Shown are data from an *in vitro* kinase assay using wild-type Sx16 or Sx16-T7A incubated with
638   MARK1 or BRSK1 kinases as described. MARK1 phosphorylated Sx16, but this was not
639   reduced in the T7A mutant and thus suggests this kinase targets a distinct site. BRSK1 was an
640   example of a kinase that did not phosphorylate Sx16.
641

Figure 1

Figure 1. Disruption of the Sx16 N-terminus perturbs GLUT4 trafficking.

HeLa cells expressing HA-GLUT4-GFP were transfected with plasmids encoding the N-terminal 33 amino acids of Sx16 fused to protein A (WT) or the same peptide with an F10A mutation, or empty plasmid (control). 48h after transfection, cells were stimulated with or without 1μM insulin for 60 minutes and fixed. Cell surface GLUT4 was immuno-stained using anti-HA (pseudo-coloured blue) in non-permeabilised cells. After washing, cells were permeabilised and cells expressing Protein-A fusions identified using a distinct secondary antibody (pseudo-coloured red). Signal from GFP is pseudo-coloured green. Shown in **Panel A** is data from a typical experiment; protein-A positive cells are indicated with a white asterisk in some panels so that transfected cells can be readily identified. **Panel B** >50 cells in each condition from four separate biological replicates were quantified to allow calculation of the HA/GFP ratio; values are expressed relative to Basal control (non-transfected) cells. *indicates a significant reduction in insulin-stimulated surface/total ratio compared to control and F10A insulin-stimulated cells (p=0.02 ANOVA).

A

BASAL | INSULIN

Control non-transfected

Sx16 N1-33

Sx16 N1-33, F10A

Sx16-PrA | Total GLUT4 (GFP) | Surface GLUT4 | Sx16-PrA | Total GLUT4 (GFP) | Surface GLUT4

B

HA/GFP ratio (fold change)

Control
WT
F10A

Basal   Insulin
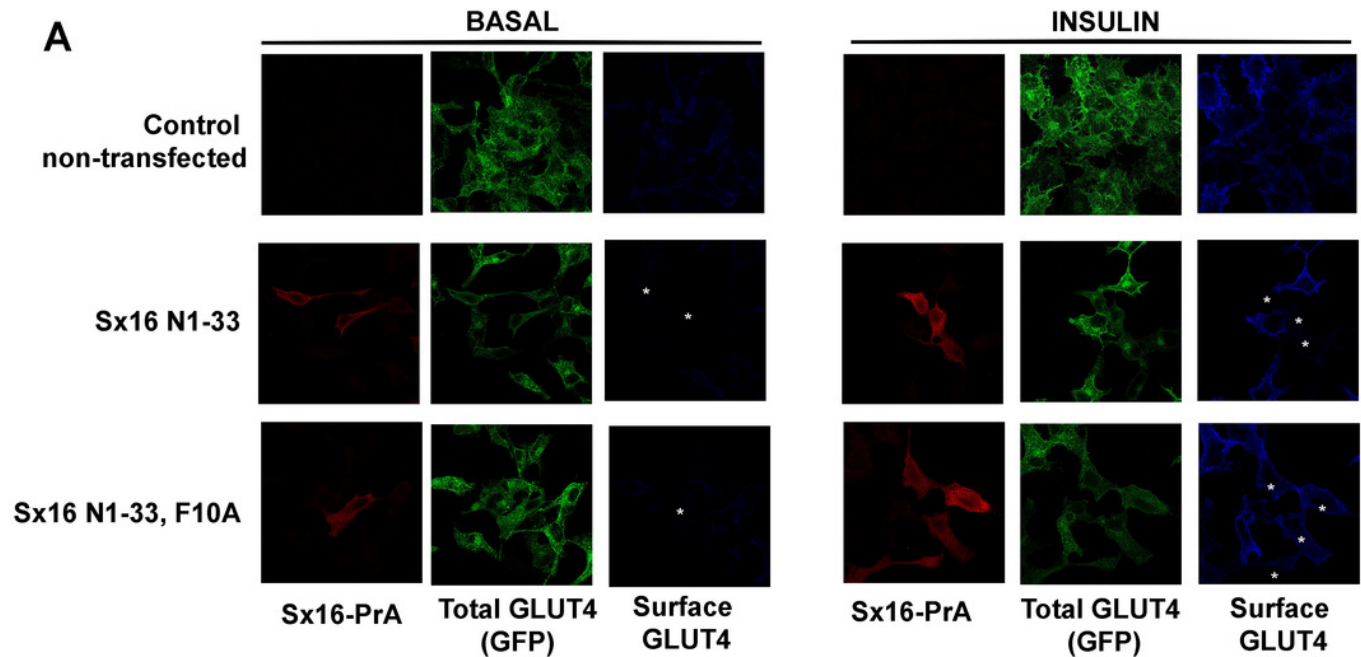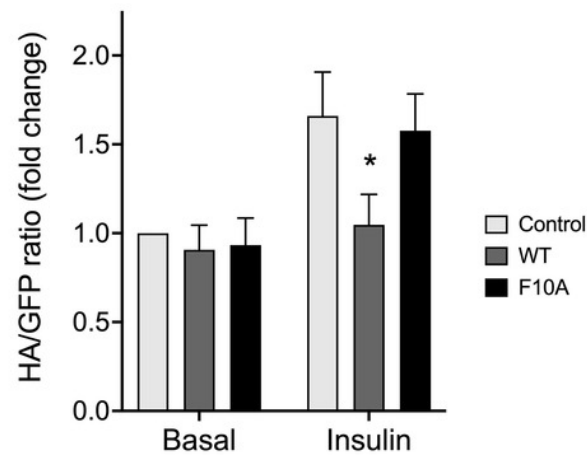
Figure 2

Figure 2. mVps45 binding to Sx16 controls GLUT4 trafficking.

HeLa cells expressing HA-GLUT4-GFP were transfected with plasmids encoding either HA-mVps45 (wild-type) or HA-mVps45-V107R (a mutant which prevents the interaction of the Sx16 N-terminus with mVps45 – see text). 48h after transfection, cells were incubated in serum-free media for 2h, fixed and cell surface GLUT4 immuno-stained using anti-HA (pseudo-coloured blue) prior to permeabilization. Subsequently, cells were permeabilised and stained using anti-mVps45 which detects both endogenous and over-expressed mVps45 (pseudo-coloured red; note that the use of HA-tagged mVps45 constructs and HA-tagged GLUT4 precluded this as a means to distinguish cells over-expressing mVps45 species). Signal from GFP is pseudo-coloured green. Shown in **Panel A** is data from a typical experiment; white asterisk represent cells expressing higher than average anti-mVps45 immunoreactivity and which are therefore assumed to be over-expressing the indicated species. Data from a typical experiment is shown. **Panel B** shows that levels of HA-GLUT4-GFP were not significantly altered upon over-expression of either wild-type or mVps45-V107R, which were expressed at similar levels (both are recognised by anti-HA); the approximate positions of molecular weight markers are shown (in kDa). **Panel C** shows quantification of the HA/GFP ratio from fields of cells such as those shown in Panel A. Fields of cells transfected with mVps45-V107R exhibited increased HA/GFP ratios compared to cells transfected with wild-type mVps45 (*p<0.001 ANOVA). Wild-type transfected cells were indistinguishable from non-transfected controls (ns; p=0.33 ANOVA). Each point on the graph is from a single field of cells; data from three independent biological experiments is presented.

A **HA-mVps45 wild type**

HA-mVps45 pocket-filled

Total mVps45
(endogenous +
over-expressed)

Total GLUT4
(GFP)

Surface GLUT4
(anti-HA)

B **Anti-HA immunoblot**

100-
75-
50-

-HA-GLUT4-GFP
-HA-mVps45

No   WT   PF
DNA

C

ns

*

Wildtype   Pocket   Control
            Filled

HA/GFP ratio (arbitrary units)

2.5

2.0

1.5

1.0

0.5
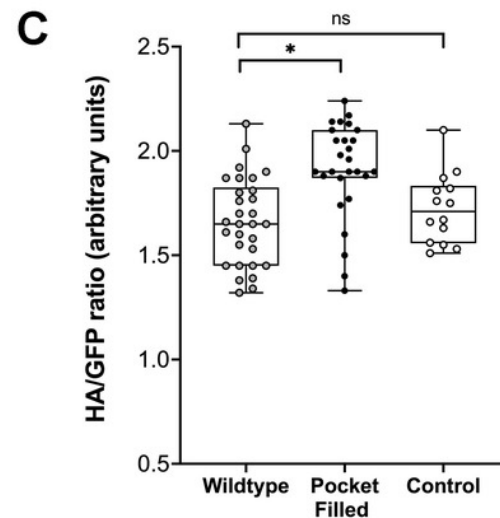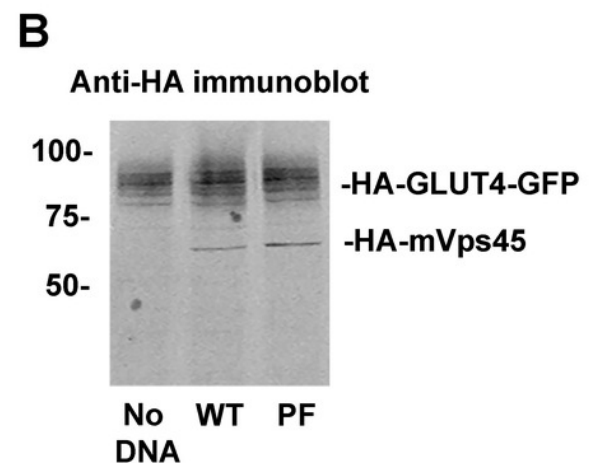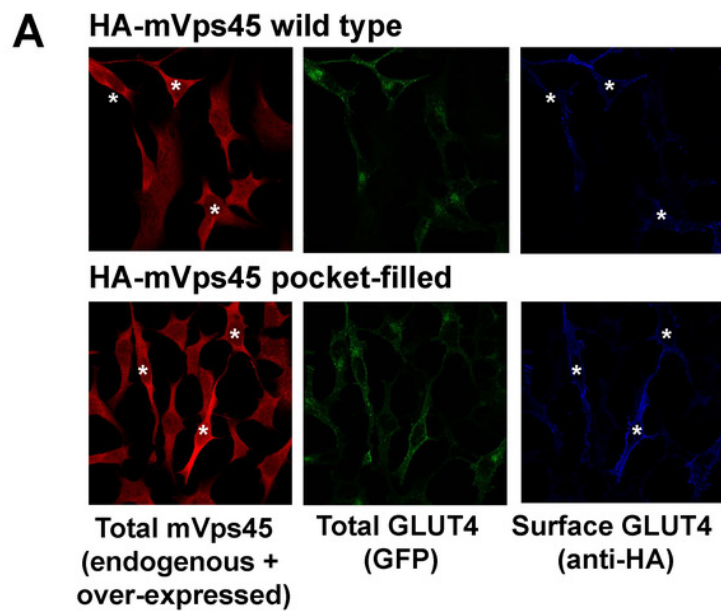
Figure 3

Figure 3. Sx16 is phosphorylated on Threonine-7.

Panel A. 3T3-L1 adipocyte cytosol was used in a series of *in vitro* kinase reactions with $[^{32}P]$ **γ**-ATP. Lane 1 shows that myelin basic protein (MBP) was efficiently phosphorylated by adipocyte cytosol. In lane 3, adipocyte cytosol phosphorylated recombinant Sx16-PrA, but did not phosphorylate PrA alone (lane 4). Lane 2 shows an identical reaction to that in lane 3 but Sx16-PrA was omitted. All lanes were run on the same gel, which has been cropped to remove either empty or irrelevant lanes; the data shown are all taken from the same exposure of the autoradiogram. This experiment was replicated with multiple batches of adipocyte cytosol with qualitatively similar results. **Panel B** shows a similar experiment in which 0.5 μg of bacterially expressed Sx16 was incubated with or without 3T3-L1 adipocyte cytosol (30 μg; 'Cytosol') in the presence or absence of 25 μM ATP for 60 minutes at 30⁰C as indicated. Samples were then immunoblotted with either anti-Sx16 antibodies ('Sx16' in figure) or anti-phospho-T7 antibodies ('Phospho-T7' Sx16 in figure). **Panel C** shows a typical immunoblot in which equal amounts of wild-type Sx16, Sx16-T7A or Sx16-T7D were separated by SDS-PAGE and immunoblotted with anti-Sx16 or anti-phospho-T7 antibodies as indicated. This experiment shows data using intact GST-fusion proteins from bacterial lysates (left lanes; 20 μg /lane) or using purified Sx16 proteins released from Glutathione beads by thrombin ('Cleaved'; right lanes, 0.5 μg/lane)). Data from a typical experiment is shown; the approximate positions of molecular weight markers are indicated (in kDa).
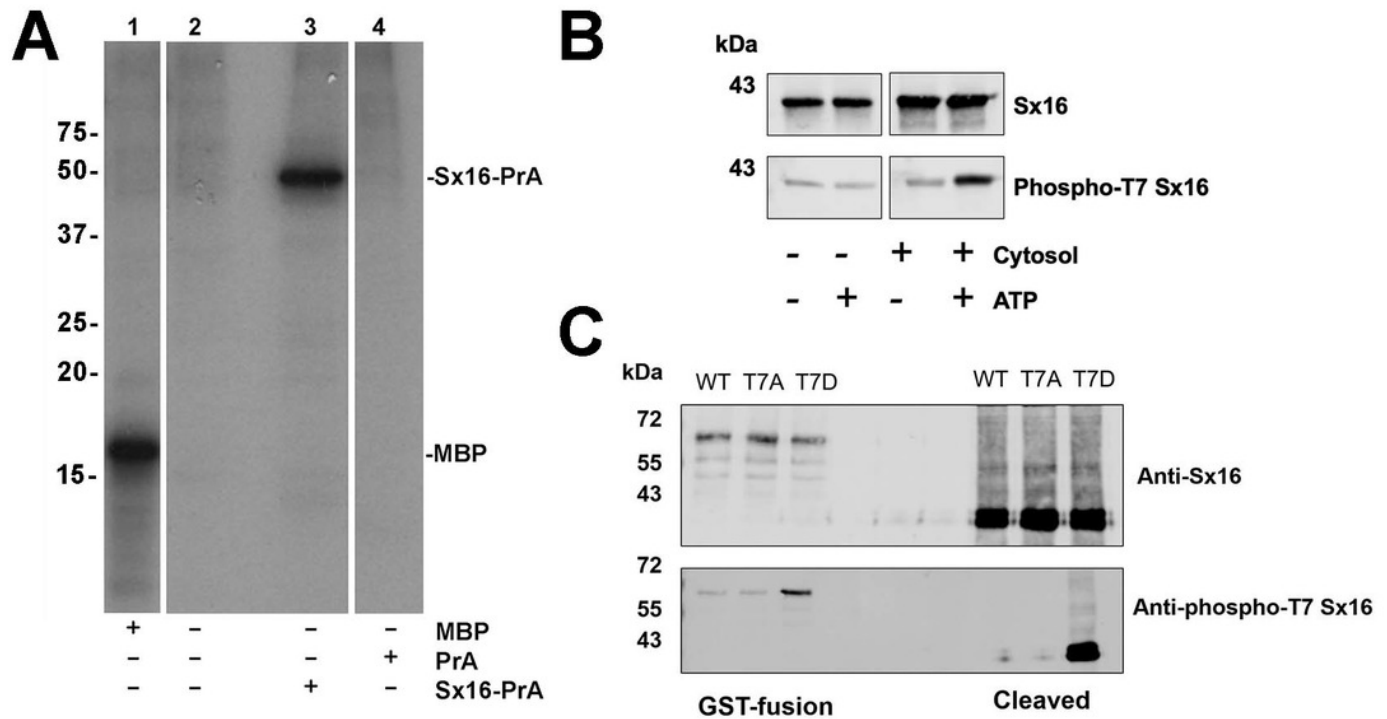
Figure 4

Figure 4. A phospho-mimetic mutation of Sx16-T7 exhibits reduced interaction with mVps45.

Identical amounts of recombinant Protein A-tagged Sx16 wild type or Sx16-T7D were used to pull down HA-tagged mVps45 over-expressed in yeast. A constant amount (250 µg) of yeast lysate expressing HA-mVps45 was incubated with decreasing amounts (20, 15, 10, 5, 2.5, and 1 µg) of either Sx16-PrA or Sx16-T7D-PrA for 2h on ice. PrA-tagged species were then captured using IgG-Sepharose beads, washed and eluted by boiling in SDS-PAGE sample buffer. Samples were then stained for total protein (**Panel A**) or immunoblotted using anti-HA (**Panel B**). In the figure, **L** refers to starting Lysate and **B** shows a sample of IgG beads (~10x more than used in the capture lanes) to control for any non-specific binding. PrA alone did not exhibit any binding to HA-mVps45 (uncropped blots can be found in the supplemental files). Data from a representative binding experiment is shown, together with quantification of three separate experiments of this type presented in **Panel C** as mean ± S.D. Note that in the quantification, the data are normalised relative to the level of mVps45 binding observed using 20 µg of Sx16. The approximate positions of molecular weight markers are indicated (in kDa).

A **Coomassie stain:**

-mVps45
-Sx16-PrA

80-
49.5-
35-
29-
20-

L B
Sx16-PrA

-mVps45
-Sx16-T7D-PrA

L B
Sx16-T7D-PrA

B **Anti-HA immunoblot:**

80-
49.5-

L B -
Sx16-PrA

-mVps45

L B -
Sx16-T7D-PrA

C

■ WT ■ T7D

mVps45 bound (% of max)

Sx16 in pull-down (μg)
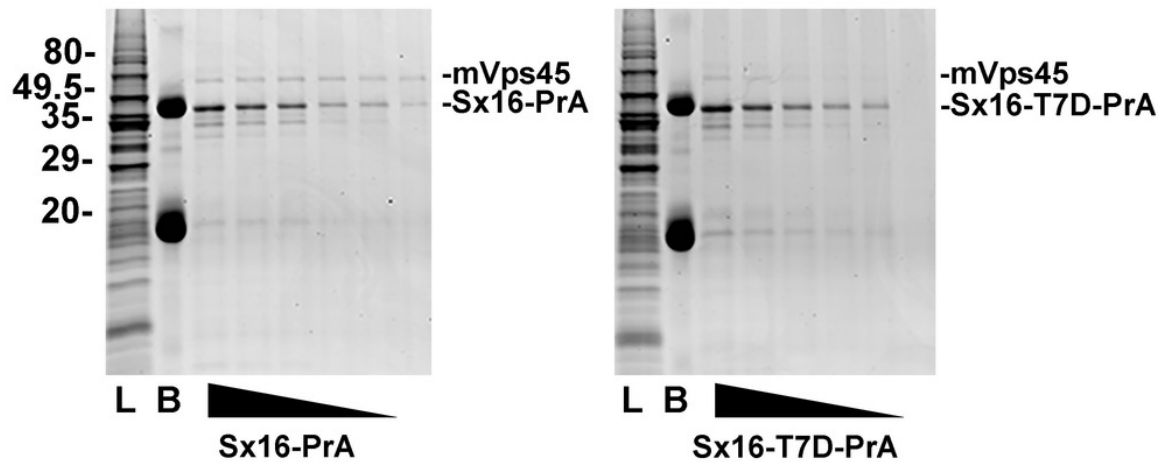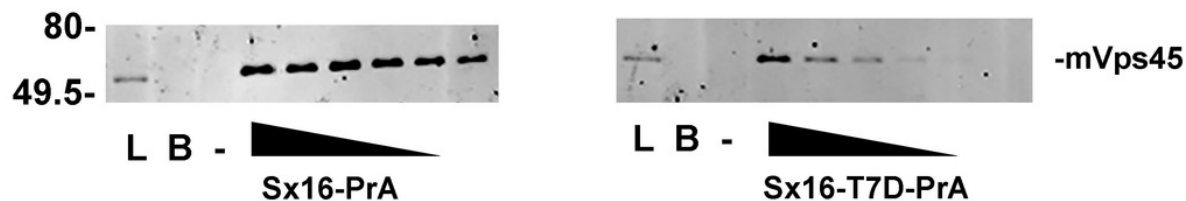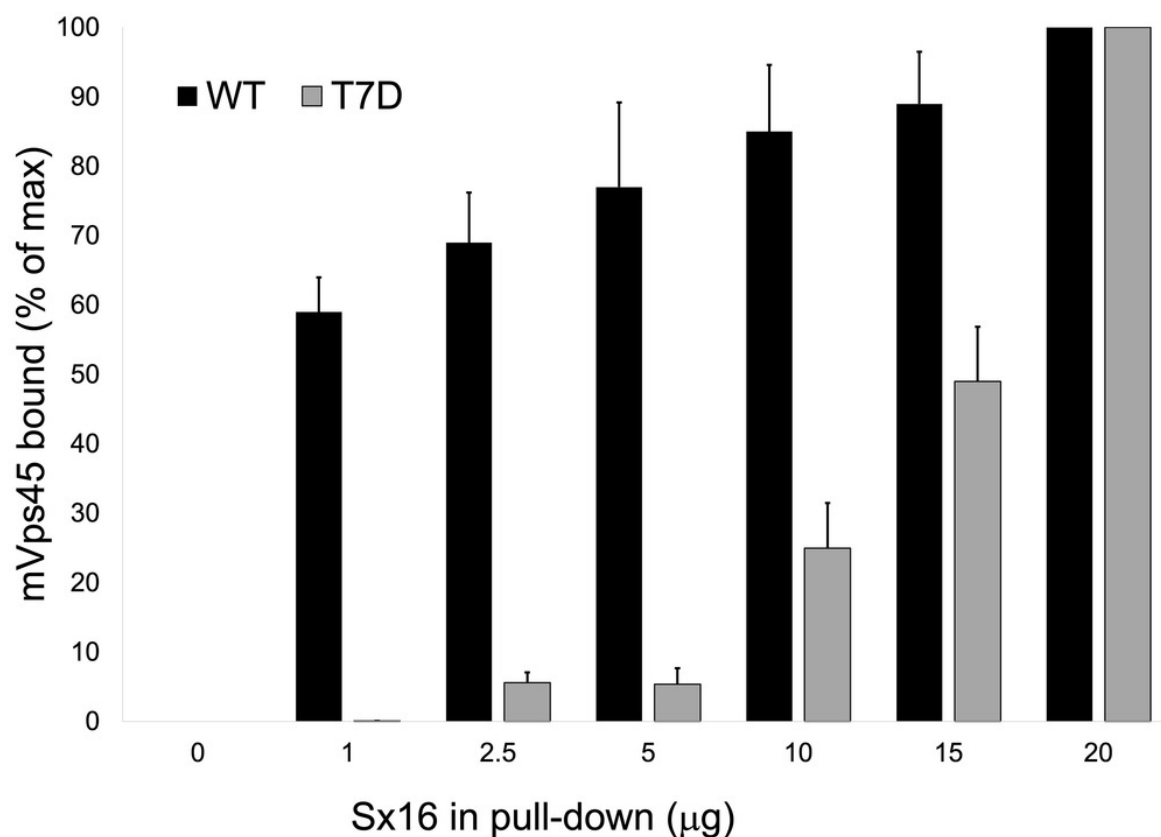
Figure 5

Figure 5. Sx16-T7D reduces insulin-stimulated glucose transport.

3T3-L1 adipocytes were infected with lentivirus delivering either wild-type Sx16, or Sx16-T7A or Sx16-T7D as outlined in *Methods*. **Panel A:** DeGlc uptake was assayed after incubation with or without 1μM insulin for 30 minutes. Shown are the means of three independent experiments in which basal and insulin-stimulated deGlc uptake rates were measured in quadruplicate at each condition and are presented as a % of the insulin-stimulated rate in control (non-infected) cells. Over-expression of Sx16-T7D consistently impaired insulin-stimulated deGlc uptake; *p=0.02 compared to control cells (ANOVA). No other differences were observed between groups. **Panel B:** Shown are lysates from a typical dataset immunoblotted with anti-Sx16, anti-GLUT4, anti-mVps45 and anti-GAPDH. Note that over-expressed Sx16 and mutants thereof consistently migrate faster than the endogenous protein (indicated by * on the figure), the approximate positions of molecular weight markers are indicated (in kDa). We saw no significant differences in levels of expression of the different Sx16 mutants across all experiments of this type. **Panel C**: 3T3-L1 adipocytes expressing either Sx16-WT, T7A or T7D (as indicated) were treated with or without 1μM insulin for 30 minutes and lysates separated on SDS-PAGE and immunoblotted using antibodies that recognise phosphorylated Akt or total Akt, as shown. Data from a typical experiment is shown.

A

B

43-
35-   - anti-Sx16
                    *
68-   - anti-mVps45

49.5-   - anti-GLUT4

35-   - anti-GAPDH

Control -
Sx16 -
Sx16 T7A -
Sx16 T7D -

C

Sx16-WT Sx16-T7A Sx16-T7D

anti-pAkt -

anti-Akt -

Insulin: -   +   -   +   -   +
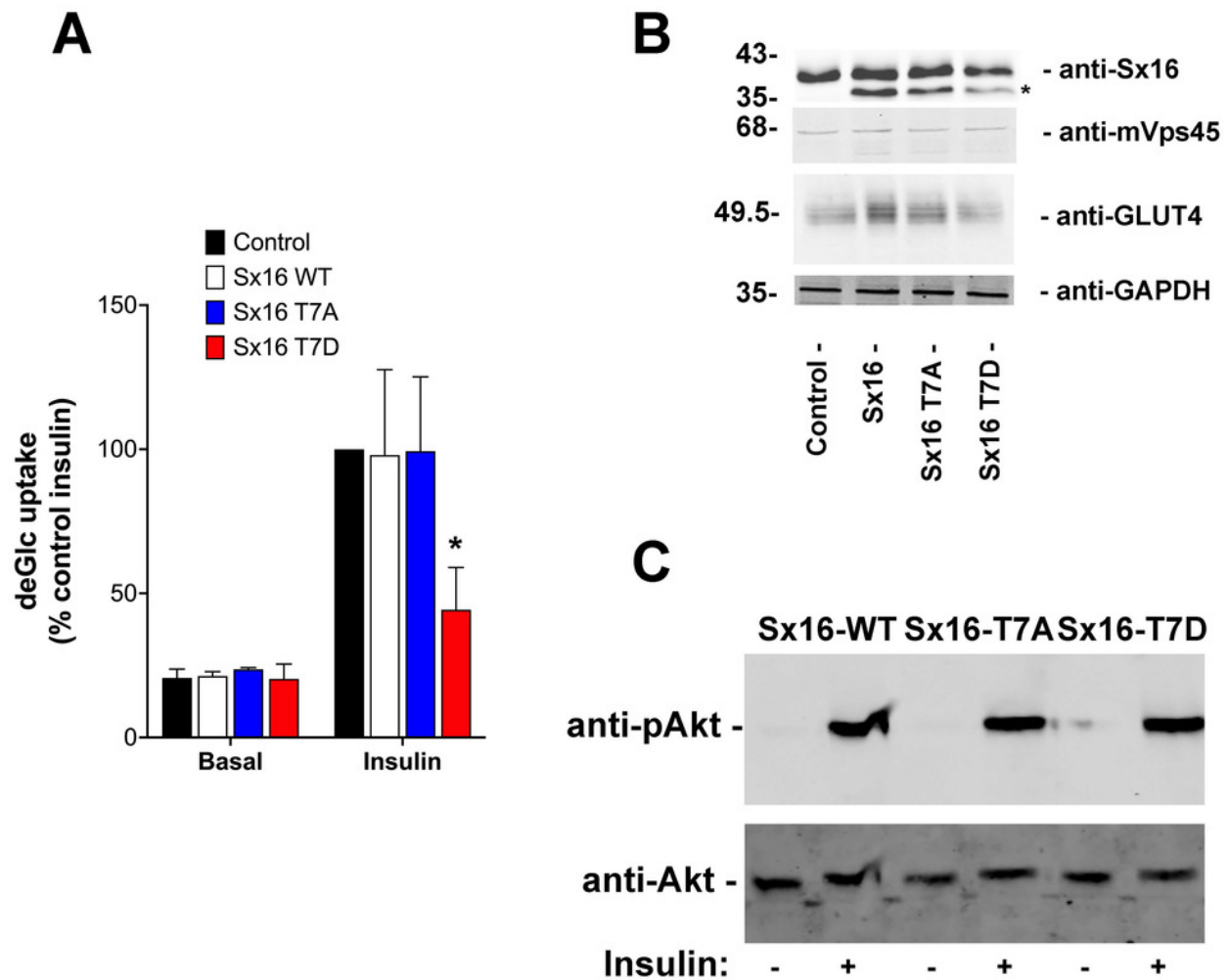
Figure 6

Figure 6. Sx16 is phosphorylated by AMPK in vitro on T7.

Purified Sx16 (WT or T7A mutant) was incubated with 5mU of either AMPK or SIK2 as indicated plus radiolabelled Mg.ATP for 30 mins at 30°C as described. The reaction was stopped by addition of 4x SDS buffer and the protein visualised following SDS-PAGE by Coomassie Staining. Phosphate incorporated into Sx16 was detected by autoradiography and quantified by excising the Sx16 bands and Cerenkov counting. A representative protein stain and autoradiogram are shown, while average (± s.e.m.) CPM incorporated in two separate experiments is provided in the bar chart. The approximate positions of molecular weight markers are indicated (in kDa).
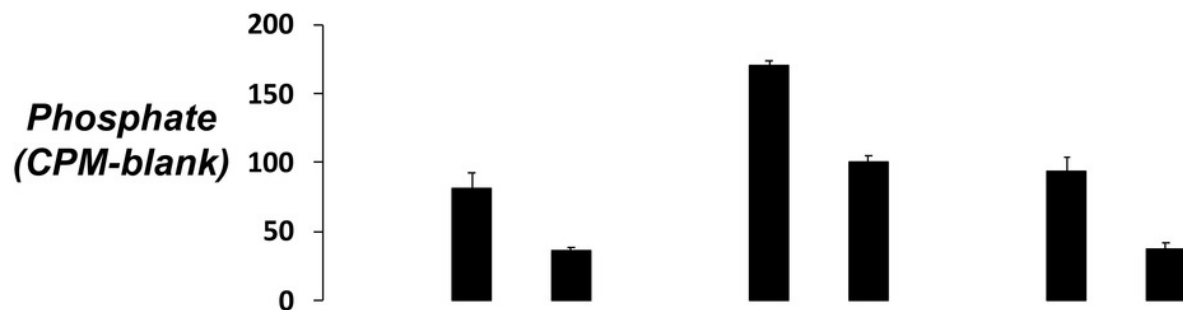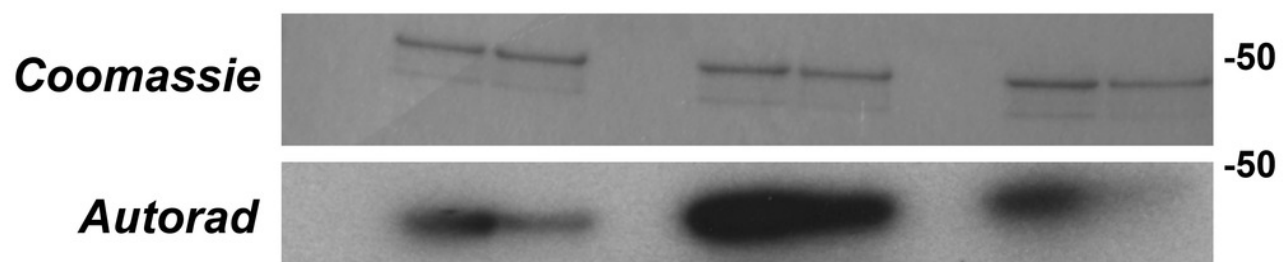
Figure 7

Figure 7. Cytosol from insulin- and AICAR-treated cells was without effect on Sx16 phosphorylation.

Panel A 0.5 µg of bacterially expressed Sx16 was incubated with 30 µg cytosol prepared from 3T3-L1 adipocytes treated without (Basal) or with 100 nM insulin as shown in the presence or absence of 25 µM ATP for 60 minutes at 30^0C as indicated. Samples were then immunoblotted with anti-Sx16 antibodies ('Sx16' in figure) or anti-phospho-T7 antibodies ('Phospho-T7' Sx16 in figure). **Panel B** shows a similar experiment to panel A except that cytosol from basal (untreated) cells was compared to cytosol prepared from cells treated with 1 mM AICAR for 60 min as indicated. As a control, cytosol was omitted from the left two lanes of this experiment. In **Panel C** Sx16 was incubated with cytosol from wild type MEFs or from MEFs lacking AMPK α1 and α2 in the presence or absence of ATP as indicated. As a control, cytosol was omitted from the left two lanes of this experiment. **Panel D** is quantification of three experiments of this type. * indicates a statistically significant difference, p=0.0064 comparing signal ATP in the presence of WT MEF cytosol by unpaired t-test. The similar comparison for AMPK KO cytosol was not significantly different; n=3 biological replicates. In all figures the approximate positions of molecular weight markers are indicated to the left of the panels (in kDa).
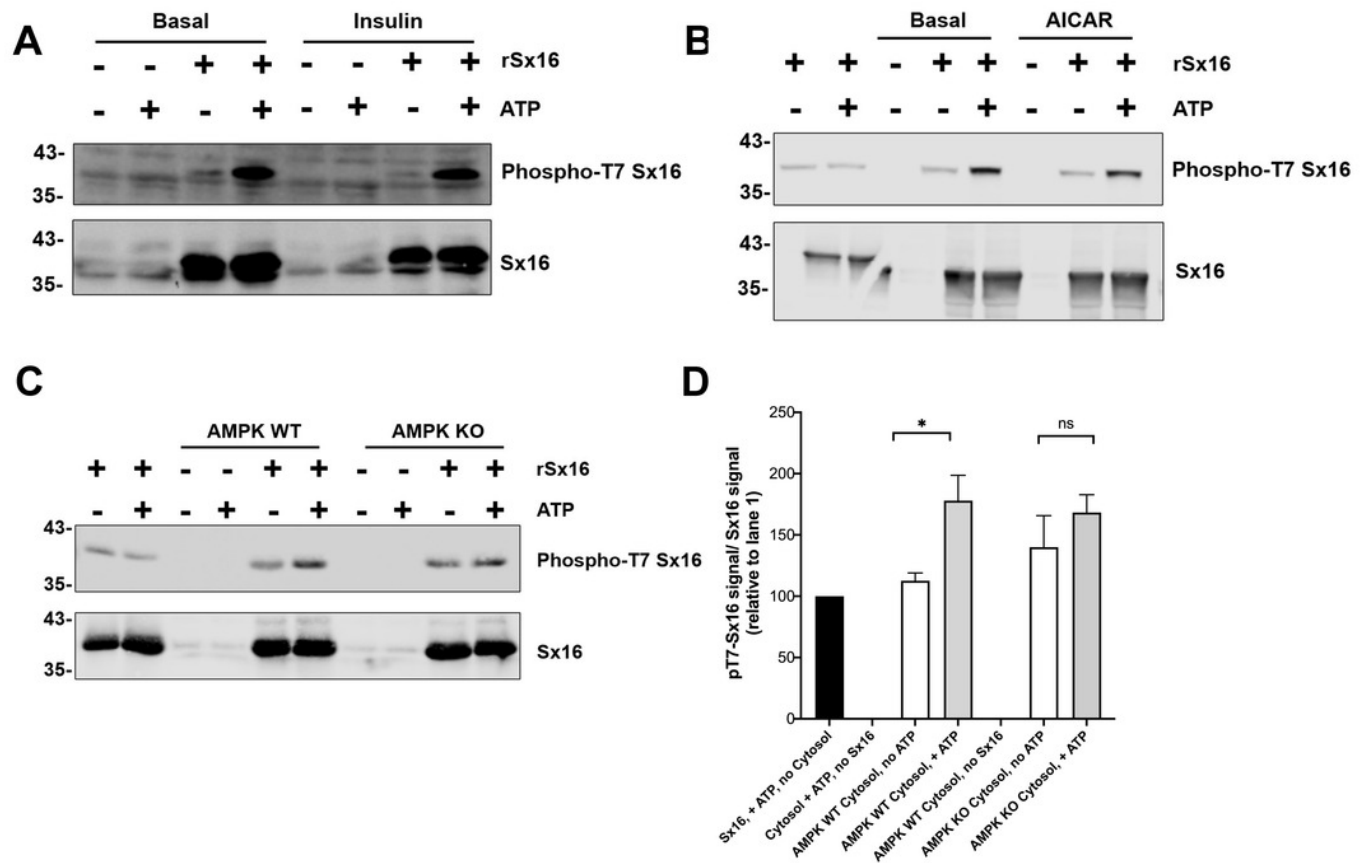
Table 1. Mascot data for phospho-site mapping identifies Thr-7 as a site of in vitro phosphorylation.

Shown are the data confirming in vitro phosphorylation of T-7. The data in italics are from a mis-cleaved peptide which also confirms the T7 site. Data was produced by the Fingerprints Facility at the University of Dundee. *The corresponding spectra are shown in Supplemental Figure 1.

1 **Table 1.**
2 **Mascot data for phospho-site mapping identifies Sx16 Thr-7 as a site of *in vitro***
3 **phosphorylation.**
4
5 Shown are the data confirming in vitro phosphorylation of Sx16 Thr-7. The data in *italics* are
6 from a mis-cleaved peptide which also confirms the T7 site. Data was produced by the
7 Fingerprints Facility at the University of Dundee. *The corresponding spectra are shown in
8 Supplemental Figure 1.
9

Spectra*	Observed	Mr (expt)	Mr (calc)	ppm	Miss	Score	Expect	Rank	Unique	Peptide
a	571.3047	1140.5948	1140.5944	0.37	0	(62)	5.8e-07	1	U	R.LTDAFLLLR.N + Phospho (ST)
b	571.3047	1140.5948	1140.5944	0.37	0	(55)	2.8e-06	1	U	R.LTDAFLLLR.N + Phospho (ST)
c	*433.2391*	*1296.6955*	*1296.6955*	*-0.00*	*1*	*(48)*	*1.6e-05*	*1*	*U*	*R.R LTDAFLLLR.N + Phospho (ST)*

12